Entrapment of Lithium Salts by the Lithium Amidinate Li[(^{n}Bu)C(N^{t}Bu)$_2$]

Tristram Chivers,* Andrew Downard, and Masood Parvez

Department of Chemistry, University of Calgary, 2500 University Drive, Calgary,
Alberta, Canada T2N 1N4

Received June 30, 1999

Four novel complexes involving lithium amidinates and lithium salts have been synthesized and crystallographically characterized. Addition of anhydrous LiX (X = OH, Cl, Br, I) to Li[(^{n}Bu)C(N^{t}Bu)$_2$] in THF afforded laddered aggregates in which two neutral lithium amidinates chelate one LiX unit. In the case of LiOH, LiCl, and LiBr, the ladders thus formed dimerize about their external LiX edges to form the complexes {(Li[(^{n}Bu)C(N^{t}Bu)$_2$])$_2$·LiX·THF}$_2$ (X = OH, Cl, Br). When the added salt is LiI, however, dimerization is apparently prevented by solvation, producing the monomeric laddered aggregate {Li[(^{n}Bu)C(N^{t}Bu)$_2$]}$_2$·LiI·2THF. In all cases, the laddered structures have a distinctive, undulating shape imparted by the conformation of the [LiNLiX] units; each three-rung ladder is composed of contiguous cisoid and transoid four-membered rings. The moieties in the dimeric species are linked by a transoid [LiX]$_2$ ring. In this way, Li[(^{n}Bu)C(N^{t}Bu)$_2$] acts as a versatile "lithio ligand" capable of chelating a variety of neutral lithium salts through electrostatic interactions. Crystal data: **3**, triclinic, space group $P\bar{1}$, $a = 13.142(4)$ Å, $b = 13.239(4)$ Å, $c = 11.425(2)$ Å, $\alpha = 94.30(2)°$, $\beta = 99.40(2)°$, $\gamma = 64.32(2)°$, $V = 1767(1)$ Å^3, $Z = 2$; **4**, monoclinic, space group $P2_1/n$, $a = 13.514(5)$ Å, $b = 11.619(6)$ Å, $c = 24.020(8)$ Å, $\beta = 99.78(4)°$, $V = 3717(3)$ Å^3, $Z = 4$; **5**, monoclinic, space group $P2_1/n$, $a = 15.163(5)$ Å, $b = 15.746(3)$ Å, $c = 17.024(6)$ Å, $\beta = 109.32(2)°$, $V = 3835.7(18)$ Å^3, $Z = 4$; **6**, monoclinic, space group $P2_1/n$, $a = 12.306(6)$ Å, $b = 18.276(8)$ Å, $c = 19.000(6)$ Å, $\beta = 96.61(4)°$, $V = 4245(3)$ Å^3, $Z = 4$.

Introduction

Over the past several years there has been growing interest in the effect of added salts in various chemical reactions.[1] The most studied and probably the most important salt effects are those caused by lithium salts (LiX).[2] This results partly from the properties of Li$^+$ and its derivatives, namely (1) Li$^+$ has the highest charge density of all the alkali-metal cations, (2) organolithium compounds and lithium salts are generally somewhat soluble in organic solvents, and (3) there are a wide variety of lithium reagents (including salts) cheaply available from commercial sources.

The ubiquity of lithio reagents is well-established in organic chemistry; to wit, it is estimated that well over 95% of contemporary natural product syntheses utilize one or more lithium-containing reagents (among them, many lithium amide bases and other N-lithiated species).[3] In addition, lithium salts are often formed as intermediates and/or byproducts in common inorganic reactions such as deprotonation,[4] amide transfer,[4] and metalation.[5] This being the case, examination of interactions between LiX salts and other species that may be present in solution (i.e., as products, reactants, or intermediates) is clearly of interest. Indeed, aggregates resulting from such interactions have been implicated as reactive intermediates in a number of cases.[3,5c,6]

N-Silylated benzamidinates have long been considered useful reagents for bidentate chelation of main group and transition metal centers,[7] and lithium amidinates are ubiquitous as sources of anionic ligands in metathetical syntheses.[8] Ostensibly intentional use of the *lithiated* species as ligands, however, is relatively rare.[9,10] Although lithium amides such as LDA[10b] and other compounds[4,5b,c,10a] have been used to trap sundry LiX fragments, we are not aware of any previous examples where lithium amidinates act in this capacity. In view of this paucity,

---

* Corresponding author. Tel: (403) 220-5741. Fax: (403) 289-9488. E-mail: chivers@ucalgary.ca.

(1) Loupy, A.; Tchoubar, B. *Salt Effects in Organic and Organometallic Chemistry*; VCH: Weinheim, Germany, 1992.

(2) Beck, A. K.; Seebach, D.; Sturder, A. In *Modern Synthetic Methods*; Ernst, B., Leumann, C., Eds.; VCH Acta: New York, 1995; p 6.

(3) Collum, D. B.; DePue, J. S. *J. Am. Chem. Soc.* **1988**, *110*, 5518.

(4) Duan, Z.; Young, V. G., Jr.; Verkade, J. G. *Inorg. Chem.* **1995**, *34*, 2179 and references therein.

(5) For examples, see: (a) Hampel, F.; Neumann, F.; Schleyer, P. v. R. *Inorg. Chem.* **1995**, *34*, 6553. (b) Bernstein, P. R.; Dorigo, A. E.; Henderson, K. W.; Williard, P. G. *Angew. Chem.* **1996**, *108*, 1420; *Angew. Chem., Int. Ed. Engl.* **1996**, *35*, 1322. (c) Clegg, W.; Edwards, A. J.; Mair, F. S.; Nolan, P. M. *Chem. Commun.* **1998**, 23 and references therein.

(6) Collum, D. B.; DePue, J. S. *J. Am. Chem. Soc.* **1988**, *110*, 5524.

(7) (a) Edelmann, F. T. *Coord. Chem. Rev.* **1994**, *137*, 403. (b) Barker, J.; Kilner, M. *Coord. Chem. Rev.* **1994**, *133*, 219.

(8) For recent examples, see: (a) Richeson, D. S.; Zhou, Y. *Inorg. Chem.* **1996**, *35*, 1423. (b) Coles, M. P.; Jordan, R. F. *J. Am. Chem. Soc.* **1997**, *119*, 8125. (c) Schoeller, W. W.; Sundermann, A.; Reiher, M. *Inorg. Chem.* **1999**, *38*, 29.

(9) Snaith, R.; Wright, D. C. In *Lithium Chemistry: A Theoretical and Experimental Overview*; Sapse, A.-M., Schleyer, P. v. R., Eds.; Wiley: New York, 1995; Chapter 8.

(10) For examples of the serendipitous isolation of LiX complexes, see: (a) Engelhardt, L. M.; Jacobsen, G. E.; Raston, C. L.; White, A. H. *Inorg. Chem.* **1991**, *30*, 3978. (b) Clegg, W.; Mair, F. S.; O'Neil, P. A. *J. Am. Chem. Soc.* **1993**, *115*, 3388. (c) Lambert, C.; Hampel, F.; Schleyer, P. v. R.; Davidson, M. G.; Snaith, R. *J. Organomet. Chem.* **1995**, *487*, 139. (d) Chivers, T.; Gao, X.; Parvez, M. *Inorg. Chem.* **1996**, *35*, 4336. (e) Batsanov, A. S.; Davidson, M. G.; Howard, J. A. K.; Lamb, S.; Lustig, C.; Price, R. D. *Chem. Commun.* **1997**, 1211. (f) Fleischer, R.; Freitag, S.; Stalke, D. *J. Chem. Soc., Dalton Trans.* **1998**, 193. (g) Fryzuk, M. D.; Giesbrecht, G. R.; Johnson, S. A.; Kickham, J. E.; Love, J. B. *Polyhedron* **1998**, *17*, 947. (h) Janssen, M. D.; Rijnberg, E.; de Wolfe, C. A.; Hogerheide, M. P.; Kruis, D.; Kooijmann, H.; Spek, A. L.; Grove, D. M.; van Koten, G. *Inorg. Chem.* **1996**, *35*, 6735. (i) van der Schaaf, P.; Hogerheide, M.; Spek, A.; Grove, D.; van Koten, G. *Chem. Commun.* **1992**, 1703.

10.1021/ic990757v CCC: $18.00 © 1999 American Chemical Society
Published on Web 08/28/1999

any new complexes which utilize these neutral "lithio ligands" to capture small molecules through electrostatic interaction are of significant interest.

Recently, we reported a sandwich complex of lithium oxide (**2**) made from the lithium amidinate $Li[(^{n}Bu)C(N^{t}Bu)_2]$ (**1**) in toluene,[11] and Mulvey and co-workers published details of a structurally related, mixed-metal (Li/Mg) complex involving benzamidinate ligands.[12] We now report that **1** can act as a lithio ligand, readily entrapping lithium salts to form laddered aggregates. The synthesis and X-ray structures of four LiX (X = OH, Cl, Br, I) complexes are described.

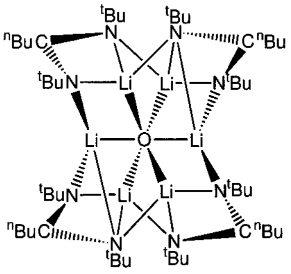

2

Experimental Section

All reactions and manipulations of air- or moisture-sensitive compounds were carried out using standard glovebox and Schlenk techniques under an atmosphere of high-purity, dried argon. The reagents $^{t}BuN{=}C{=}N^{t}Bu$ and $^{n}BuLi$ (2.5 M in hexanes) were obtained from Aldrich and used as received. The lithium salts LiX (X = Cl, Br, I) and $LiOH{\cdot}H_2O$, also obtained from Aldrich, were ground and dried for a minimum of 2 h at ≥150 °C under vacuum before use. The reagent **1** was prepared by the addition of $^{n}BuLi$ to an equimolar amount of $^{t}BuN{=}C{=}N^{t}Bu$ in toluene at 296 K.[11,13] Solvents were purchased commercially and distilled prior to use. Toluene, tetrahydrofuran, and hexane were distilled twice over a mixture of sodium metal and benzophenone. Pentane was distilled over sodium metal. Deuterated solvents (benzene-d_6 and toluene-d_8) were purchased in predried ampules and degassed using three freeze/thaw cycles prior to use. All solvents were stored over molecular sieves in glass flasks equipped with Teflon needle valves and hose-joint sidearms.

^{1}H and ^{13}C NMR spectra were obtained by using a 5 mm probe in a Bruker ACE200 200 MHz instrument equipped with a TecMag (Macintosh) software interface. Chemical shifts are reported relative to TMS in benzene-d_6. A Bruker AM400 400 MHz instrument with a 10 mm multinuclear probe and Aspect 3000 software was used for variable-temperature ^{7}Li NMR solution studies, and chemical shifts are reported relative to 1 M LiCl in D_2O. Measurements of carbon, nitrogen, and hydrogen content (by percent) in samples were performed on a Control Equipment Corp. (CEC) 440 elemental analyzer by the Analytical Services Laboratory, Department of Chemistry, University of Calgary. Fourier transform infrared (FTIR) spectra were obtained on a Mattson Genesis Series instrument.

Preparation of $\{(Li[(^{n}Bu)C(N^{t}Bu)_2])_2{\cdot}LiOH{\cdot}THF\}_2$ (3). Anhydrous LiOH (0.041 g, 1.72 mmol) was added to $Li[(^{n}Bu)C(N^{t}Bu)_2]$ (0.744 g, 3.41 mmol), a yellow powder, in a pear-shaped Schlenk vessel. Addition of THF (7 mL) at 23 °C produced a clear yellow solution with some precipitate. This was stirred for 48 h at 23 °C. On cessation of stirring, the reaction mixture was white and opalescent with no obvious precipitate. Removal of excess THF under dynamic vacuum yielded a dry, dull white powder. Total yield of solid identified as $\{(Li[(^{n}Bu)C(N^{t}Bu)_2])_2{\cdot}LiOH{\cdot}THF\}_2$ was 89% (0.809 g, 0.759 mmol). Crystals suitable for analysis by X-ray diffraction were obtained from saturated solutions of hexane or pentane after several days at room temperature. Mp: 48−50 °C (clear liquid). Anal. Calcd for $C_{30}H_{63}N_4Li_3O_2$: C, 67.65; H, 11.92; N, 10.52. Found: C, 67.62; H, 12.40; N, 10.52. IR (KBr, Nujol mull), ν (cm^{-1}): 3677, 2727, 1515, 1356, 1272, 1217, 1190, 1081, 1053, 898, 829, 801, 595, 559, 477, 445. ^{1}H NMR (200 MHz, benzene-d_6, 25 °C, δ(TMS in $CDCl_3$)), δ: 3.5−3.6 (m, 4H, THF), 2.5−2.7 (m, 4H, $-CH_2CH_2CH_2CH_3$), 1.7−1.9 (m, 4H, $-CH_2CH_2CH_2CH_3$), 1.43 (s, 32H, $-C(CH_3)_3$; m, 4H, THF), 1.3−1.4 (m, 4H, $-CH_2CH_2CH_2CH_3$), 0.96 (t, 6H, $-CH_2CH_2CH_2CH_3$). ^{13}C NMR (50.288 MHz, benzene-d_6, 25 °C, δ(TMS in $CDCl_3$)), δ: 179.4 (s, $(^{n}Bu)C(N^{t}Bu)_2$), 68.2 (s, THF), 51.5 (s, $-C(CH_3)_3$), 33.6 (s, $-C(CH_3)_3$, $-CH_2CH_2CH_2CH_3$, $-CH_2CH_2CH_2CH_3$), 25.3 (s, THF), 24.1 (s, $-CH_2CH_2CH_2CH_3$), 14.4 (s, $-CH_2CH_2CH_2CH_3$). ^{7}Li NMR (116.54 MHz, benzene-d_6, 25 °C, δ(1 M LiCl in D_2O)), δ: −0.70.

Preparation of $\{(Li((^{n}Bu)C(N^{t}Bu)_2])_2{\cdot}LiCl{\cdot}THF\}_2$ (4). Dry LiCl (0.049 g, 1.16 mmol) was placed in a pear-shaped Schlenk vessel with $Li[(^{n}Bu)C(N^{t}Bu)_2]$ (0.504 g, 2.31 mmol). Addition of THF (10 mL) at 23 °C gave a clear yellow solution with a small amount of white precipitate. The mixture was allowed to stir for 18 h, during which a clear, virtually colorless solution developed. Removal of solvent in vacuo produced a dry yellow powder, which was washed with hexane (2 × 5 mL). Total yield of solid identified as $\{(Li[(^{n}Bu)C(N^{t}Bu)_2])_2{\cdot}LiCl{\cdot}THF\}_2$ was 92% (0.585 g, 0.531 mmol). Crystals suitable for analysis by X-ray diffraction were obtained from the hexane washings after storage at −14 °C for several days. Mp: 128−132 °C (decomposition to an orange solid); 290−293 °C (dark orange liquid). Anal. Calcd for $C_{30}H_{62}N_4ClLi_3O$: C, 65.38; H, 11.34; N, 10.17. Found: C, 65.82; H, 10.98; N, 11.14. IR (KBr, Nujol mull), ν (cm^{-1}): 2727, 1652, 1272, 1201, 1047, 894, 826, 800, 644, 507. ^{1}H NMR (200 MHz, benzene-d_6, 25 °C, δ(TMS in $CDCl_3$)), δ: 3.6−3.8 (m, 4H, THF), 2.5−2.7 (m, 4H, $-CH_2CH_2CH_2CH_3$), 1.9−2.1 (m, 4H, $-CH_2CH_2CH_2CH_3$), 1.50 (s, 32H, $-C(CH_3)_3$), 1.3−1.5 (m, 4H, THF), 0.99 (t, 6H, $-CH_2CH_2CH_2CH_3$). ^{13}C NMR (50.288 MHz, toluene-d_8, 7 °C, δ(TMS in $CDCl_3$)), δ: 179.2 (s, $(^{n}Bu)C(N^{t}Bu)_2$), 68.8 (s, THF), 51.4 (s, $-C(CH_3)_3$), 34.9 (s, $-C(CH_3)_3$, 32.8 (s, $-CH_2CH_2CH_2CH_3$), 29.6 (s, $-CH_2CH_2CH_2CH_3$), 25.9 (s, THF), 24.3 (s, $-CH_2CH_2CH_2CH_3$), 14.9 (s, $-CH_2CH_2CH_2CH_3$). ^{7}Li NMR (155.508 MHz, toluene-d_8, δ(1 M LiCl in D_2O)): at 25 °C, δ: −1.69 (s); at −33 °C, δ: −1.24 (s), −1.68 (s), −2.41 (s).

Preparation of $\{(Li[(^{n}Bu)C(N^{t}Bu)_2])_2{\cdot}LiBr{\cdot}THF\}_2$ (5). Dry LiBr (0.101 g, 1.16 mmol) and $Li[(^{n}Bu)C(N^{t}Bu)_2]$ (0.498 g, 2.28 mmol) were dissolved in THF (10 mL) at 23 °C to give a clear yellow solution. After 18 h of stirring, no further changes in the reaction mixture were observed. Removal of excess solvent under dynamic vacuum yielded a dry yellow powder, which, after being washed with pentane (2 × 5 mL), pumped down to a white powder. Total yield of solid identified as $\{(Li[(^{n}Bu)C(N^{t}Bu)_2])_2{\cdot}LiBr{\cdot}THF\}_2$ was 95% (0.642 g, 0.539 mmol). Crystals suitable for analysis by X-ray diffraction were obtained from the pentane washings after storage at −14 °C overnight. Mp: 158−160 °C (clear yellow liquid). Anal. Calcd for $C_{30}H_{62}BrLi_3O$: C, 60.50; H, 10.49; N, 9.41. Found: C, 60.15; H, 10.95; N, 9.19. IR (KBr, Nujol mull), ν (cm^{-1}): 2727, 1653, 1302, 1262, 1222, 1198, 1044, 890, 825, 801. ^{1}H NMR (200 MHz, benzene-d_6, 25 °C, δ(TMS in $CDCl_3$)), δ: 3.6−3.8 (m, 4H, THF), 2.5−2.7 (m, 4H, $-CH_2CH_2CH_2CH_3$), 1.8−2.1 (m, 4H, $-CH_2CH_2CH_2CH_3$), 1.52 (s, 32H, $-C(CH_3)_3$), 1.3−1.5 (m, 4H, THF), 0.98 (t, 6H, $-CH_2CH_2CH_2CH_3$). ^{13}C NMR (50.288 MHz, toluene-d_8, 7 °C, δ(TMS in $CDCl_3$)), δ: 179.4 (s, $(^{n}Bu)C(N^{t}Bu)_2$), 69.3 (s, THF), 51.9 (s, $-C(CH_3)_3$), 34.5 (s, $-C(CH_3)_3$), 34.2 (s, $-CH_2CH_2CH_2CH_3$), 33.9 (s, $-CH_2CH_2CH_2CH_3$), 25.8 (s, THF), 24.3 (s, $-CH_2CH_2CH_2CH_3$), 14.9 (s, $-CH_2CH_2CH_2CH_3$). ^{7}Li NMR (155.508 MHz, toluene-d_8, δ(1M LiCl in D_2O)): at 25 °C, δ: −1.79 (s); at −53 °C, δ: −1.16 (s), −1.70 (s), −2.60 (s).

Preparation of $(Li[(^{n}Bu)C(N^{t}Bu)_2])_2{\cdot}LiI{\cdot}2THF$ (6). Dry LiI (0.257 g, 1.92 mmol) and $Li[(^{n}Bu)C(N^{t}Bu)_2]$ (0.838 g, 3.84 mmol) were dissolved in THF (10 mL) to give a clear yellow solution. This was stirred for 4 h at 23 °C, during which no change was observed. Removal of excess THF in vacuo yielded an oily yellow solid. This was dissolved in hexane (10 mL) to give a clear yellow solution, which subsequently pumped down to a fine, dry, yellow powder. Total yield of solid identified as $\{Li[(^{n}Bu)C(N^{t}Bu)_2]\}_2{\cdot}LiI{\cdot}2THF$ was 95% (1.176 g, 0.915

---

(11) Chivers, T.; Downard, A.; Yap, G. P. A. *J. Chem. Soc., Dalton Trans.* **1998**, 2603.

(12) Kennedy, A. R.; Mulvey, R. E.; Rowlings, R. B. *J. Am. Chem. Soc.* **1998**, *120*, 7816.

(13) Chivers, T.; Downard, A.; Yap, G. P. A. *Inorg. Chem.* **1998**, *37*, 5708.

Table 1. Selected Bond Lengths (Å) and Angles (deg) in **3**−**6**

3		**4**		**5**		**6**	
O(1)−Li(1)	1.967(9)	Cl(1)−Li(1)	2.390(11)	Br(1)−Li(1)	2.56(2)	I(1)−Li(1)	2.741(11)
O(1)−Li(2)	2.018(8)	Cl(1)−Li(2)	2.304(11)	Br(1)−Li(2)	2.59(2)	I(1)−Li(2)	2.797(11)
O(1)−Li(3)	1.918(9)	Cl(1)−Li(3)	2.502(14)	Br(1)−Li(3)	2.68(3)	I(1)−Li(3)	2.979(13)
O(1)−Li(3*)	2.081(8)	Cl(1)−Li(2*)	2.412(12)	Br(1)−Li(2*)	2.46(2)		
O(2)−Li(1)	2.046(17)	O(1)−Li(1)	1.931(13)	O(1)−Li(1)	1.93(2)	O(1)−Li(1)	1.917(12)
						O(2)−Li(2)	1.942(11)
Li(3*)−N(1)	2.068(9)	Li(1)−N(2)	1.957(13)	Li(1)−N(2)	1.98(3)	Li(1)−N(1)	2.033(12)
Li(2)−N(2)	2.055(9)	Li(2)−N(3)	1.978(12)	Li(2)−N(3)	1.94(2)	Li(2)−N(4)	1.992(12)
Li(2)−N(4)	2.029(9)	Li(3)−N(4)	1.985(15)	Li(3)−N(4)	2.02(3)	Li(3)−N(2)	2.066(12)
Li(1)−N(3)	2.018(10)	Li(3)−N(1)	1.987(15)	Li(3)−N(1)	1.98(3)	Li(3)−N(3)	2.031(12)
Li(3*)−N(2)	2.100(9)	Li(1)−N(1)	2.082(13)	Li(1)−N(1)	2.11(3)	Li(1)−N(2)	2.047(12)
Li(1)−N(4)	2.136(9)	Li(2)−N(4)	2.053(13)	Li(2)−N(4)	2.02(3)	Li(2)−N(3)	2.081(12)
C(1)−N(1)	1.322(6)	C(1)−N(1)	1.350(7)	C(1)−N(1)	1.385(16)	C(1)−N(1)	1.330(8)
C(1)−N(2)	1.340(6)	C(1)−N(2)	1.311(7)	C(1)−N(2)	1.314(17)	C(1)−N(2)	1.349(8)
C(14)−N(3)	1.313(6)	C(14)−N(4)	1.359(7)	C(14)−N(4)	1.328(16)	C(14)−N(3)	1.359(7)
C(14)−N(4)	1.361(6)	C(14)−N(3)	1.326(7)	C(14)−N(3)	1.303(16)	C(14)−N(4)	1.324(8)
N(1)−C(1)−N(2)	111.8(4)	N(1)−C(1)−N(2)	112.5(6)	N(1)−C(1)−N(2)	116.3(15)	N(1)−C(1)−N(2)	112.0(5)
N(1)−C(1)−C(2)	125.3(5)	N(1)−C(1)−C(2)	123.9(6)	N(1)−C(1)−C(2)	119.5(15)	N(1)−C(1)−C(2)	124.2(6)
C(2)−C(1)−N(2)	122.7(5)	C(2)−C(1)−N(2)	123.4(6)	C(2)−C(1)−N(2)	123.7(15)	C(2)−C(1)−N(2)	123.5(6)
N(3)−C(14)−N(4)	114.4(4)	N(3)−C(14)−N(4)	112.4(6)	N(3)−C(14)−N(4)	112.6(16)	N(3)−C(14)−N(4)	113.1(5)
N(3)−C(14)−C(15)	123.8(5)	N(3)−C(14)−C(15)	124.6(7)	N(3)−C(14)−C(15)	123.0(17)	N(3)−C(14)−C(15)	122.6(5)
C(15)−C(14)−N(4)	121.5(4)	C(15)−C(14)−N(4)	122.8(6)	C(15)−C(14)−N(4)	124.2(15)	C(15)−C(14)−N(4)	124.1(5)

Table 2. Crystallographic Data for **3**−**6**

	3	**4**	**5**	**6**
empirical formula	$C_{30}H_{63}N_4O_2Li_3$	$C_{30}H_{62}N_4OLi_3Cl$	$C_{30}H_{62}N_4OLi_3Br$	$C_{34}H_{70}N_4O_2Li_3I$
fw	532.68	551.12	595.57	714.68
T, K	170(1)	170(1)	170(1)	170(1)
crystal system	triclinic	monoclinic	monoclinic	monoclinic
space group	$P\bar{1}$ (No. 2)	$P2_1/n$ (No. 14)	$P2_1/n$ (No. 14)	$P2_1/n$ (No. 14)
a, Å	13.142(4)	13.514(5)	15.163(5)	12.306(6)
b, Å	13.239(4)	11.619(6)	15.746(3)	18.276(8)
c, Å	11.425(2)	24.020(8)	17.024(6)	19.000(6)
α, deg	94.30(2)	90.000	90.000	90.000
β, deg	99.40(2)	99.78(4)	109.32(2)	96.61(4)
γ, deg	64.32(2)	90.000	90.000	90.000
V, Å^3	1767(1)	3717(3)	3835.7(18)	4245(3)
Z	2	4	4	4
ρ_{calcd}, g cm^{-3}	1.001	0.985	1.031	1.118
abs coeff, cm^{-1}	0.61	1.27	10.8	7.84
F_{000}	592	1216	1288	1520
crystal size, mm	0.50 × 0.40 × 0.40	0.62 × 0.50 × 0.39	0.50 × 0.48 × 0.20	0.38 × 0.35 × 0.32
$2\theta_{max}$, deg	50.1	55.2	40.0	55.1
no. of reflns collected	6556	9412	4161	10567
no. of independent reflns	6257	9042	3884	9770
R_{int}	0.064	0.062	0.04	0.083
data [$I > 2\sigma(I)$]/parameters	1857/363	2527/353	1226/317	4300/409
GOF	0.981	3.04	1.63	1.024
residuals: *R*,[a] R_w	0.0671, 0.1837[b]	0.061, 0.071[c]	0.047, 0.045[c]	0.0529, 0.1418[d]

[a] $R = \sum||F_o| - |F_c||/\sum|F_o|$. [b] $w = 1/[\sigma^2|F_o| + (0.1235P)^2]$; $P = (F_o^2 + 2F_c^2)/3$. [c] $R_w = [\sum w(|F_o| - |F_c|)^2/\sum wF_o^2]^{1/2}$. [d] $w = 1/[\sigma^2|F_o| + (0.0584P)^2 + 17.2683P]$; $P = (F_o^2 + 2F_c^2)/3$.

mmol). Crystals suitable for analysis by X-ray diffraction were obtained from hexane after storage at −14 °C overnight. Mp: 93−96 °C (clear yellow liquid). Anal. Calcd for $C_{34}H_{70}N_4ILi_3O_2$: C, 56.08; H, 9.72; N, 8.72. Found: C, 56.37; H, 10.00; N, 8.42. IR (KBr, Nujol mull), *ν* (cm^{-1}): 2725, 1652, 1305, 1262, 1198, 1048, 1019, 918, 893, 873, 825, 800, 640, 561, 509. ^{1}H NMR (200 MHz, benzene-d_6, 25 °C, *δ*(TMS in $CDCl_3$)), *δ*: 3.6−3.8 (m, 8H, THF), 2.5−2.8 (m, 4H, $-\mathrm{C}H_2\mathrm{CH_2CH_2CH_3}$), 1.8−2.1 (m, 4H, $-\mathrm{CH_2C}H_2\mathrm{CH_2CH_3}$), 1.50 (s, 32H, $-\mathrm{C(C}H_3)_3$), 1.3−1.5 (m, 8H, THF), 0.97 (t, 6H, $-\mathrm{CH_2CH_2CH_2C}H_3$). ^{13}C NMR (50.288 MHz, toluene-d_8, 7 °C, *δ*(TMS in $CDCl_3$)), *δ*: 179.0 (s, (^{n}Bu)*C*(N^{t}Bu)$_2$), 69.8 (s, THF), 51.8 (s, $-C\mathrm{(CH_3)_3}$), 34.4 (s, $-\mathrm{C(}C\mathrm{H_3)_3}$), 33.9 (s, $-C\mathrm{H_2CH_2CH_2CH_3}$), 33.5 (s, $-\mathrm{CH_2}C\mathrm{H_2CH_2CH_3}$), 25.9 (s, THF), 24.1 (s, $-\mathrm{CH_2CH_2}C\mathrm{H_2CH_3}$), 14.6 (s, $-\mathrm{CH_2CH_2CH_2}C\mathrm{H_3}$). ^{7}Li NMR (155.508 MHz, toluene-d_8, *δ*(1 M LiCl in D_2O)): at 25 °C, *δ* = −2.05 (s); at 7 °C, *δ* = −1.82 (s), −2.15 (s); at −33 °C, *δ* = −1.67 (s), −2.25 (s), −2.76 (s).

X-ray Measurements. Data were collected at low temperature using oil or epoxy-coated crystals mounted on glass fibers. All measurements were made on a Rigaku AFC6S diffractometer with graphite-monochromated Mo Kα radiation (*λ* = 0.710 69 Å). Empirical absorption corrections were applied in each case.[14] Selected bond distances and angles are given in Table 1, and relevant crystallographic data are presented in Table 2.

3. The structure was solved by direct methods[15] and expanded using Fourier techniques.[16] The THF atoms were disordered over two sites with unequal site occupancy factors. Non-hydrogen atoms were refined anisotropically with the exception of the carbon atoms of THF, which were refined isotropically. Hydrogen atoms were included but not refined. The hydrogen atom attached to O(1) was located from a

---

(14) North, A. T. C.; Phillips, D. C.; Mathews, F. S. *Acta Crystallogr.* **1968**, *A24*, 351.

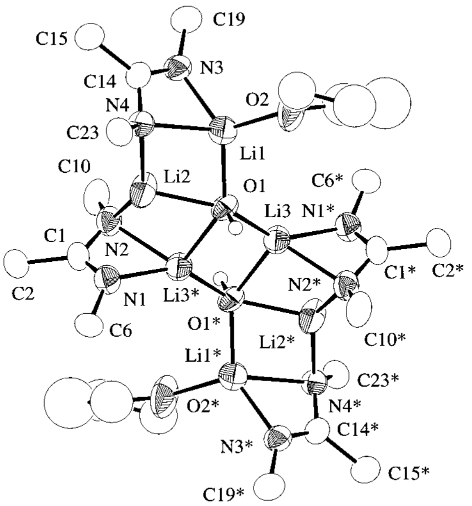

Figure 1. ORTEP diagram of $\{(\mathrm{Li}[(^n\mathrm{Bu})\mathrm{C}(\mathrm{N}^t\mathrm{Bu})_2])_2\cdot\mathrm{LiOH}\cdot\mathrm{THF}\}_2$ (**3**) showing the atom-labeling scheme. Thermal ellipsoids are depicted at 50% probability; for clarity, only the α-carbon atoms of *tert*-butyl and *n*-butyl groups are shown.

difference map and included in the refinement at that position. Full-matrix least-squares refinement on F^2 was performed using SHELX97.[17]

4. The structure was solved by direct methods[18] and expanded using Fourier techniques.[16] The non-hydrogen atoms were refined anisotropically. Hydrogen atoms were included at geometrically idealized positions (with $d(\mathrm{C-H}) = 0.95$ Å) but not refined. Full-matrix least-squares refinement was performed using teXsan.[19]

5. The structure was solved and expanded using Fourier techniques.[16] The lithium atoms and the carbon atoms of THF were refined isotropically while all other non-hydrogen atoms were refined anisotropically. Hydrogen atoms were included at geometrically idealized positions (with $d(\mathrm{C-H}) = 0.95$ Å) but not refined. Full-matrix least-squares refinement was performed using teXsan.[19]

6. The structure was solved by direct methods[15] and expanded using Fourier techniques.[16] All non-hydrogen atoms were refined anisotropically except C(29) and C(30) (these atoms were disordered and allowed to refine isotropically over two sites each with partial occupancy factors). Hydrogen atoms were included but not refined. Full-matrix least-squares refinement on F^2 was performed using SHELX97.[17]

Results and Discussion

Preparation and Structure of $\{(\mathrm{Li}[(^n\mathrm{Bu})\mathrm{C}(\mathrm{N}^t\mathrm{Bu})_2])_2\cdot\mathrm{LiOH}\cdot\mathrm{THF}\}_2$ (3). In the lithium oxide complex **2**, dimeric lithium amidinate ladders act as ligands in the entrapment of a $\mathrm{Li_2O}$ molecule;[11] LiOH could not be trapped by **1** in toluene because protonation of the lithio ligand occurred, producing $\mathrm{Li_2O}$ in situ, eventually yielding **2**. This is apparently not true when the same reaction is undertaken in a coordinating solvent. A mixture of anhydrous LiOH with 2 equiv of **1** in THF at room temperature formed a clear yellow solution that yielded a white solid on removal of solvent. An X-ray structural determination revealed that the composition of the recrystallized product was $\{(\mathrm{Li}[(^n\mathrm{Bu})\mathrm{C}(\mathrm{N}^t\mathrm{Bu})_2])_2\cdot\mathrm{LiOH}\cdot\mathrm{THF}\}_2$ (**3**, Figure 1).

Unlike the case of the corresponding reaction of LiOH with **1** in toluene to produce **2** (eq 1), the presence of THF apparently prevents protonation of **1** by LiOH and allows facile isolation of the hydroxide-containing complex (eq 2). Indeed, attempts

$$\underset{\mathbf{1}}{5\mathrm{Li}[(^n\mathrm{Bu})\mathrm{C}(\mathrm{N}^t\mathrm{Bu})_2]} + \mathrm{LiOH} \xrightarrow{\text{toluene}} \underset{\mathbf{2}}{\{\mathrm{Li}[(^n\mathrm{Bu})\mathrm{C}(\mathrm{N}^t\mathrm{Bu})_2]\}_4\cdot\mathrm{Li_2O}} + {}^t\mathrm{BuN{=}C(NH^tBu)(^nBu)} \quad (1)$$

$$\underset{\mathbf{1}}{4\mathrm{Li}[(^n\mathrm{Bu})\mathrm{C}(\mathrm{N}^t\mathrm{Bu})_2]} + 2\mathrm{LiOH} \xrightarrow{\text{THF}} \underset{\mathbf{3}}{\{(\mathrm{Li}[(^n\mathrm{Bu})\mathrm{C}(\mathrm{N}^t\mathrm{Bu})_2])_2\cdot\mathrm{THF}\cdot\mathrm{LiOH}\}_2} \quad (2)$$

to deprotonate **3** using ^{n}BuLi (and, hence, generate **2**) were unsuccessful, suggesting that the hydroxyl proton is relatively inert. This is probably due to the steric protection offered by ^{n}Bu, ^{t}Bu, and THF substituents, all of which hinder access to the central $[\mathrm{LiOH}]_2$ portion of the molecule.

In contrast to the structure of **2**, where $\mathrm{Li_2O}$ is chelated by *dimeric* lithium amidinates, the structure of **3** can be understood in a formal sense as chelation of LiOH by solvated, *monomeric* lithium amidinates (Figure 2). The reagent **1** acts as a lithio ligand, chelating LiOH to produce a three-rung ladder which subsequently loses one solvent molecule and dimerizes by laddering about Li−O edges to give **3**. An alternative, perhaps more likely, route to **3** involves co-complexation of a $(\mathrm{LiOH})_2$ dimer with the dimeric lithium amidinate. The aggregate acquires its distinctive shape (S_4 symmetry) by virtue of the conformation adopted by each of the [LiNLiO] units. The structure is best described by considering cisoid and transoid orientations about the four-membered rings involved. This terminology was originally coined to describe the orientation of substituents in four-membered amido−lithium rings containing primary or asymmetric secondary amides;[20] the terms are used here in a more general sense to describe the orientation of any three contiguous (edge-sharing) four-membered rings with respect to one another (Figure 3). In cases where the amido substituent R^1 is a pendant arm which binds to the metal (lithium) cation at the β-position, the two usages are in fact identical.

Each three-rung ladder in **3** is composed of contiguous cisoid and transoid four-membered rings, an arrangement which minimizes steric congestion among the various substituents present and imparts a gentle undulation to the structure as a whole. The halves of the dimer are linked by a transoid $[\mathrm{LiO}]_2$ ring. In solution, **3** appears to possess greater symmetry than it does in the solid state; ^{1}H and ^{13}C NMR spectra measured at room temperature are consistent with single environments for the ligands, and only a single peak is seen in the ^{7}Li NMR spectrum. Solid-state NMR is not an effective investigative tool in this case, as the broad peaks obtained make resolution of near-coincident signals impossible.

Examination of the metrical parameters for **3** (see Table 1) reveals an unanticipated asymmetry in the amidinate ligands. Although the observed C−N distances within the [NCN] units of the amidinates are consistent with delocalized π-bonding throughout, one C−N bond in each ligand is somewhat shorter than the other [$d(\mathrm{C(1)-N(1)}) = 1.322(6)$ Å versus $d(\mathrm{C(1)-N(2)}) = 1.340(6)$ Å; $d(\mathrm{C(14)-N(3)}) = 1.313(6)$ Å versus

---

(15) SIR92: Altomare, A.; Cascarano, M.; Giacovazzo, C.; Guagliardi, A. *J. Appl. Crystallogr.* **1993**, *26*, 343.

(16) DIRDIF94: Beurskens, P. T.; Admiraal, G.; Beurskens, G.; Bosman, W. P.; de Gelder, R.; Israel, R.; Smits, J. M. M. *The DIRDIF-94 program system*; Technical Report; Crystallography Laboratory, University of Nijmegen: Nijmegen, The Netherlands, 1994.

(17) SHELX97: Sheldrick, G. M. *Program for the Refinement of Crystal Structures*; University of Gottingen: Gottingen, Germany, 1997.

(18) SAPI91: Hai-Fu, F. *Structure Analysis Programs with Intelligent Control*; Rigaku Corp.: Tokyo, 1991.

(19) teXsan: *Crystal Structure Analysis Package*; Molecular Structure Corp.: The Woodlands, TX, 1985 and 1992.

(20) Clegg, W.; Henderson, K. W.; Horsburgh, L.; Mackenzie, F. M.; Mulvey, R. E. *Chem. Eur. J.* **1998**, *4*, 53.

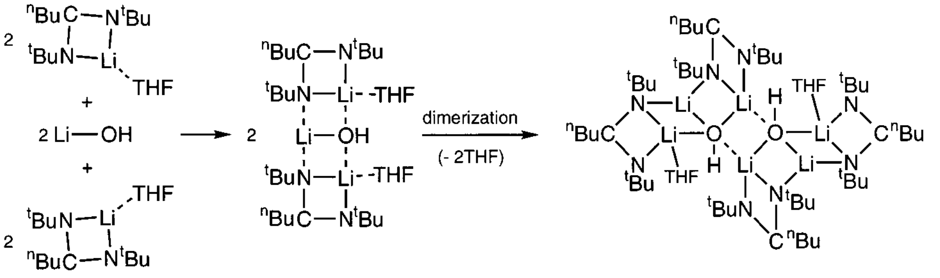

Figure 2. Chelation of LiOH by solvated, monomeric lithium amidinates, showing partial desolvation resulting from dimerization.

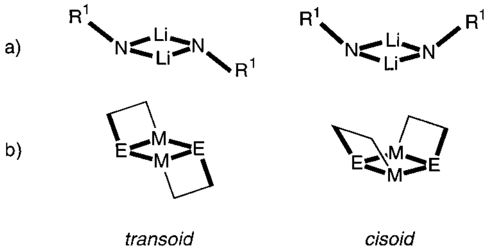

Figure 3. Cisoid and transoid orientations in (a) primary (or asymmetric, secondary) lithium amides and (b) arrays of three contiguous four-membered rings.

d(C(14)−N(4)) = 1.361(6) Å]. The shorter bonds involve 3-coordinate N atoms, and the longer ones, 4-coordinate N atoms. This effect is significant in only one of the amidinate moieties; it is much less pronounced in the other due to a long-range interaction between N(1) and Li(2) [d(N(1)$\cdots$Li(2)) = 2.353 Å], effectively raising the coordination number of both atoms involved (a similar long-range contact is observed in **2**[11]). Presumably Li(2) remains unsolvated due to steric hindrance provided by two bulky N^{t}Bu neighbors. The Li−O distances in **3** are unremarkable [|d(Li−O)| = 1.980 Å; range 1.918(9)−2.081(8) Å (solvent contacts excluded)].

The Li−N distances around the outside of the ladder show no significant variation and are slightly shorter than the Li−N distances across the "rungs" [|d(Li−N)| = 2.042 Å versus 2.118 Å]. The geometries about C(1) and C(14) are essentially planar [$\Sigma(\angle C)$ = 359.8 and 359.7°, respectively]. As was observed for **2**, the internal NCN angles of the amidinate ligands [|$\angle$NCN| = 113.1(4)°] are smaller than their external counterparts [|$\angle$NCC| = 123.3(5)°]. The hydroxyl proton of **3** was located and included in the refinement [d(O(1)−H(1)) = 1.051 Å].

Although complexes of LiOH with a lithio ligand[21] and with other main group centers[22] have been reported, we are not aware of any previous examples which are formed by simple addition of the two reagents. Thus, despite being quite self-evident, the directed synthesis presented here apparently has not been used to prepared lithio ligand/LiOH adducts. More commonly, hydrolysis of a lithio reagent is employed to produce LiOH in situ, which then undergoes complexation. For example, Roesky et al. have deliberately hydrolyzed ^{n}BuLi in THF to prepare the adducts E(Mes)$_3$·LiOH·3THF (E = Al, Ga).[22] In a related preparation, Lambert and co-workers isolated the aggregate {Li[O^{t}Bu]}$_{10}$·[LiOH]$_6$ from a concentrated solution of Li[O^{t}Bu] in hexane after prolonged exposure to moist air.[21] The latter complex comprises two hexagonal prismatic Li$_6$[(O^{t}Bu)$_5$(OH)] units linked by a crossed LiOH ladder framework. The Li−O distances in the LiOH portion of this molecule are somewhat longer [|d(Li−O)| = 2.145 Å] than those observed in **3**. The two values are not directly comparable, however, since O(1) is 5-coordinate in **3**, whereas four 3-coordinate and two 6-coordinate oxygen atoms are present in the LiOH ladder framework of {Li[O^{t}Bu]}$_{10}$·[LiOH]$_6$.

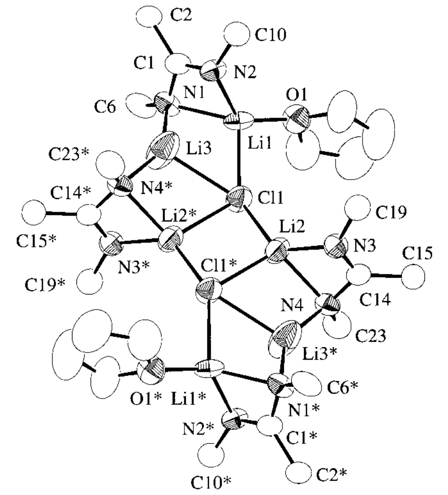

Figure 4. ORTEP diagram of {(Li[(^{n}Bu)C(N^{t}Bu)$_2$])$_2$·LiCl·THF}$_2$ (**4**) showing the atom-labeling scheme. Thermal ellipsoids are depicted at 50% probability; for clarity, only the α-carbon atoms of *tert*-butyl and *n*-butyl groups are shown.

In light of these past reports, we have verified that **3** can also be produced in ca. 75% yield by quantitative hydrolysis of **1** in THF (eq 3).

$$\underset{\mathbf{1}}{6Li[(^nBu)C(N^tBu)_2]} + 2H_2O \xrightarrow{THF} \underset{\mathbf{3}}{\{(Li[(^nBu)C(N^tBu)_2])_2\cdot THF\cdot LiOH\}_2} + 2\,^tBuN{=}C(NH^tBu)(^nBu) \quad (3)$$

Preparation and Structure of {(Li[(^{n}Bu)C(N^{t}Bu)$_2$])$_2$·LiX·THF}$_2$ (4, X = Cl; 5, X = Br). Given that **1** can act as a lithio ligand to entrap Li$_2$O or LiOH, reactions with other LiX salts are clearly germane to a more detailed understanding of the phenomenon. The methodology used to synthesize **3** was successfully employed to isolate and characterize the novel species {(Li[(^{n}Bu)C(N^{t}Bu)$_2$])$_2$·LiX·THF}$_2$ (**4**, X = Cl; **5**, X = Br) from the reactions of **1** with LiCl and LiBr, respectively. Both compounds are approximately isostructural with **3** (Figures 4 and 5).

The average Li−Br distance in **5** [|d(Li−Br)| = 2.57 Å] is 0.17(2) Å longer than the average Li−Cl distance in **4** [|d(Li−Cl)| = 2.402 Å], a 7.0% increase consistent with the predicted lengthening of 0.15 Å[23] (cf. |d(Li−O)| = 1.980 Å in **3**). These lithium−halide distances are similar to those observed in previous lithio ligand/LiX complexes (cf. |d(Li−Br)| = 2.608

---

[21] Davidson, M. G.; Hampel, F.; Lambert, C.; Schleyer, P. v. R.; Snaith, R. *J. Organomet. Chem.* **1995**, *487*, 139.

[22] Storre, J.; Schnitter, C.; Roesky, H. W.; Schmidt, H.-G.; Noltemeyer, M.; Fleischer, R.; Stalke, D. *J. Am. Chem. Soc.* **1997**, *119*, 7505.

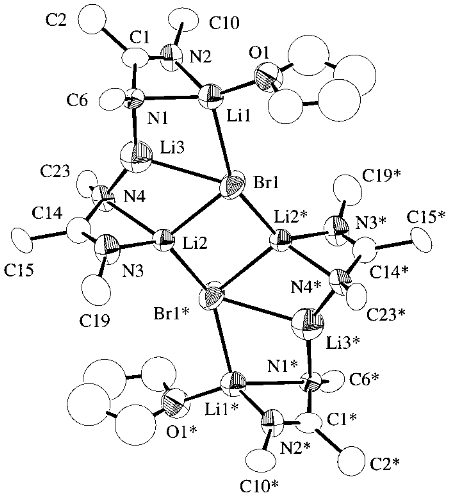

Figure 5. ORTEP diagram of $\{(\mathrm{Li}[(^n\mathrm{Bu})\mathrm{C}(\mathrm{N}^t\mathrm{Bu})_2])_2\cdot\mathrm{LiBr}\cdot\mathrm{THF}\}_2$ (**5**) showing the atom-labeling scheme. Thermal ellipsoids are depicted at 50% probability; for clarity, only the α-carbon atoms of *tert*-butyl and *n*-butyl groups are shown.

Å in $\mathrm{Li[N(SiMe_3)_2]\cdot\{Li[OC(^tBu){=}CH_2]\}_2\cdot LiBr\cdot 2TMEDA}$[5b] and $|d(\mathrm{Li{-}Cl})| = 2.409$ Å in $\mathrm{\{Li[N(^iPr)_2]\}_2\cdot LiCl\cdot 2TMEDA}$[10b] and 2.389 Å in $\mathrm{[Li_2H_4\{(Me_3SiNCH_2CH_2)_3N\}_2]\cdot LiCl}$[4]).

The Li−N distances around the outside of the ladders are virtually identical [$|d(\mathrm{Li{-}N})| = 1.977$ Å for **4** and 1.98 Å for **5**] and, as with **3**, are slightly shorter than the Li−N distances across the "rungs" [$|d(\mathrm{Li{-}N})| = 2.067$ Å for **4** and 2.06 Å for **5**]. Although the C−N bond distances within the [NCN] units of the amidinate ligands in **4** and **5** suggest delocalized π-bonding, bonds involving 3-coordinate N atoms are again shorter [$|d(\mathrm{C{-}N})| = 1.318$ Å for **4** and 1.308 Å for **5**] than those involving 4-coordinate N atoms [$|d(\mathrm{C{-}N})| = 1.354$ Å for **4** and 1.356 Å for **5**]. As was observed for **3**, long-range interactions between Li(3) and N(3) [$d(\mathrm{Li(3)\cdots N(3)}) = 2.962$ Å for **4** and 2.637 Å for **5**] stabilize these formally 3-coordinate centers. Geometries about the central carbon atoms of the amidinate ligands are planar in all cases [$\sum(\angle \mathrm{C}) =$ ca. 360°] with the internal N−C−N angles being somewhat less than 120° [$|\angle\mathrm{NCN}| = 112.4(6)°$ in **4** and 114.4(16)° in **5**]. Solvent contacts are similar in the two molecules with $d(\mathrm{Li{-}O}) = 1.931(13)$ Å for **4** and 1.93(2) Å for **5**.

As was the case with **3**, compounds **4** and **5** appear to possess higher average symmetry in solution than in the solid state; ^{1}H, ^{7}Li, and ^{13}C NMR spectra in solution at room temperature suggest single environments for the ligands. Variable-temperature NMR studies revealed three environments for Li atoms at low temperatures, as would be expected from the observed solid-state structures.

Preparation and Structure of $\{\mathrm{Li[(^nBu)C(N^tBu)_2]}\}_2\cdot\mathrm{LiI}\cdot 2\mathrm{THF}$ (6). Unlike its isoelectronic counterparts [LiX; X = OH, Cl, Br], LiI reacted with **1** to produce a *monomeric* aggregate (C_2 symmetry) solvated by *two* molecules of THF. Addition of LiI to 2 equiv of **1** in THF yielded a yellow oil which was rendered crystalline by the addition of hexane. An X-ray structural determination of the material after recrystallization from pentane revealed that the composition of the crystals was $\{\mathrm{Li[(^nBu)C(N^tBu)_2]}\}_2\cdot\mathrm{LiI}\cdot 2\mathrm{THF}$ (**6**) (Figure 6).

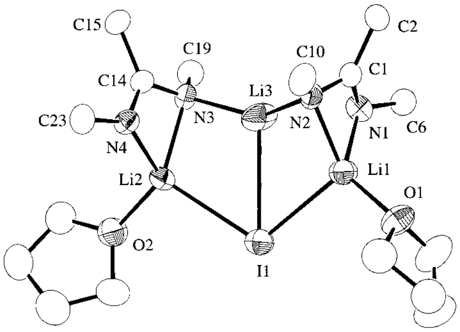

Figure 6. ORTEP diagram of $\{\mathrm{Li[(^nBu)C(N^tBu)_2]}\}_2\cdot\mathrm{LiI}\cdot 2\mathrm{THF}$ (**6**) showing the atom-labeling scheme. Thermal ellipsoids are depicted at 50% probability; for clarity, only the α-carbon atoms of *tert*-butyl and *n*-butyl groups are shown.

The structure of **6** is comparable to half of the dimeric arrangement adopted by **3**−**5**. In this case, however, solvation of a second lithium center on the same side of the three-rung ladder is apparently preferred over dimerization as a mechanism to disperse electronic charge. Presumably solvation is thermodynamically favored over dimerization in the case of LiI due to the relatively weaker Li−I bonds as reflected in the low lattice enthalpy ($\Delta H_\mathrm{L} = 761$ kJ mol^{-1}; cf. 852 kJ mol^{-1} for LiCl and 815 kJ mol^{-1} for LiBr).[24] The sites of solvation in **6** are evidently directed by steric factors; the unsolvated lithium center is hindered by two adjacent N^{t}Bu groups, whereas the two solvated centers have only one such bulky neighbor.

The overall shape of the three-rung ladder in six **6** is similar to that observed for **3**−**5**. The Li(3)−I(1) bond forming the middle rung of the ladder system is significantly longer [2.979(13) Å] than the other two Li−I bonds [$d(\mathrm{Li(1){-}I(1)}) = 2.741(11)$ Å, $d(\mathrm{Li(2){-}I(1)}) = 2.797(11)$ Å]; as a consequence, the average Li−I distance in **6** [$|d(\mathrm{Li{-}I})| = 2.839$ Å] is 0.26 Å longer than the average Li−Br distance in **5** (cf. a predicted lengthening of 0.19 Å based on covalent radii).[23] Although somewhat shorter than that recently reported for the triazasulfite/LiI complex $\mathrm{Li_2[S(N^tBu)_3]\cdot LiI\cdot 3THF}$ [$|d(\mathrm{Li{-}I})| = 2.944$ Å],[10f] the average Li−I distance in **6** is longer than those reported for the arenethiolate complex $\mathrm{Li[SC_6H_3\text{-}2,6\text{-}(CH_2NMe_2)]\cdot LiI\cdot 2THF}$[10h] and the related species $\mathrm{\{Li[OC_6H_2\text{-}2,6\text{-}(CH_2NMe_2)_2\text{-}4\text{-}Me]\cdot LiI\}_2}$[10i] [$|d(\mathrm{Li{-}I})| = 2.760$ and 2.776 Å, respectively]. The related complex $\mathrm{\{[2\text{-}Me(py)]\cdot LiI\}_2}$ contains a $\mathrm{[LiI]_2}$ ring with distances similar to those observed in **6** [$d(\mathrm{Li{-}I}) = 2.821(10)$ Å].[25]

Interestingly, there is no significant difference between Li−N bond lengths in the rungs of **6** [$|d(\mathrm{Li{-}N})| = 2.064$ Å] and those around the outside of the ladder [$|d(\mathrm{Li{-}N})| = 2.029$], suggesting that this effect may arise as a consequence of dimerization in **3**−**5**. A long-range contact between N(1) and Li(3) [$d(\mathrm{N(1)\cdots Li(3)}) = 2.388$ Å] again accounts for a slight variation in C−N bond lengths, although the effect is not as pronounced as in the cases previously discussed. The geometries about C(1) and C(14) are again planar [$\sum(\angle\mathrm{C(1)}) = 359.7°$, $\sum(\angle\mathrm{C(14)}) = 359.8°$], and the internal NCN angles at these atoms are smaller [$|\angle\mathrm{NCN}| = 112.5(5)°$] than the exterior angles [$|\angle\mathrm{NCC}| = 123.6(6)°$].

Solution NMR data for **6** indicate single environments for the amidinate ligands, suggesting higher average symmetry than in the solid state. On cooling, the singlet observed in the ^{7}Li NMR spectrum at room temperature splits first into two signals (as would be expected for the solid-state structure) and then into three. The latter behavior is similar to that observed for

---

(23) Pauling, L. *The Nature of the Chemical Bond*, 3rd ed.; Cornell University Press: Ithaca, NY, 1960; p 224.

(24) Atkins, P.; Langford, C.; Shriver, D. *Inorganic Chemistry*; 2nd ed.; Freeman: New York, 1994; p 128.

(25) Raston, C. L.; Whitaker, C. R.; White, A. H. *J. Chem. Soc., Dalton Trans.* **1988**, 991.

3−**5**; it may indicate that dimerization occurs in solution at lower temperatures although this seems unlikely since it would involve dissociation of one THF ligand.

Conclusion

In summary, we have shown that the lithium amidinate **1** can be used to chelate lithium salts, generating novel laddered aggregates. Whereas *dimeric* lithium amidinate ladders act as ligands in noncoordinating solvents (e.g., **2**), solvated *monomeric* units appear to be the active ligands in THF. Since many syntheses make use of steps which generate lithium salts in situ, we suggest that the use of **1** (or similar compounds) as a lithio ligand to entrap small polar molecules may offer a new perspective for examining the many salt−substrate interactions that undoubtedly occur in common reaction chemistry. Thus, the complexation of lithium amidinates and related species with alkali-metal salts is an interesting possibility worthy of future study.

Acknowledgment. We thank the NSERC (Canada) for financial support and the University of Calgary for a Silver Anniversary Fellowship (A.D.).

Supporting Information Available: X-ray crystallographic files, in CIF format, for complexes **3**−**6**. This material is available free of charge via the Internet at http://pubs.acs.org.

IC990757V